JOURNAL OF MARITIME RESEARCH

Vol XXIII. No. I (2026) pp 105–114

ISSN: 1697-4840, www.jmr.unican.es

Study of the Weather Impact Conditions on Fire Risk (Tank Fire) at the Condensate Storage Farm in the RTO Marine Terminal

Yassine Boudjemaa[1,*], Amine Morsli[1], Kadda Boumediene[2]

ARTICLE INFO

Article history:
Received 17 Oct 2025;
in revised from 25 Nov 2025;
accepted 16 Dec 2025.

Keywords:
Thermal radiation flux, effect distance, statistical analysis, correlation analysis, nonlinear models, meteorological impact.

ABSTRACT

This study presents an in-depth analysis of the impact of meteorological conditions (temperature, humidity, and wind speed) on the effect distance, represented here by the thermal radiation flux generated by a tank fire at the condensate terminal of the Western Regional Pipeline Transport Directorate (RTO), which is located in the Arzew industrial zone and operated by Sonatrach Oil Company Major. The meteorological data used, covering the period from 2019 to 2024 (15,000 data points), were analysed by using advanced statistical techniques and predictive models to provide accurate and reliable insights. The results indicate that the view factor is the most influential variable affecting the thermal radiation flux, which plays a critical role in determining the impact distance, accounting for 94.97% of the variance in the multiple regression model. Wind speed and inclination angle have a moderate impact, approximately 1.8% and 1.3% respectively, while other variables such as temperature, humidity, and emissivity have a negligible effect (1.3×10^{-5}, 0.3% and 0% respectively).
Correlation analysis between the studied parameters and the thermal flux reveals strong positive correlations for the factor view and the inclination angle, with coefficients of 0.995 and 0.625, respectively, moderate values for wind speed (0.371) and atmospheric transmissivity (0.0186) and negligible values for temperature, humidity, emissivity and flame height. Finally, the multiple regression model demonstrates excellent performance with an R^2 value of 0.9996. Moreover, the very low standard error (0.0376), the high F-statistic (5,646,171.787) and a p-value of 0 confirm the model's high precision and strong statistical significance.

1. Introduction.

The determination of effect distances associated with thermal fluxes emitted by pool fires of flammable liquids is a multidisciplinary issue that requires combining knowledge in thermodynamics, fluid mechanics, and numerical modelling.

The statistical analysis of the impact of meteorological conditions (temperature, wind speed, and air humidity) on thermal flux (directly) and on effect distance (indirectly), is crucial for understanding the interactions between these variables and the thermal flux, as well as for developing a reliable predictive model.

In this context, several studies have been carried out:

Samia Chettouh et al. (2016) [1] conducted a statistical study on accidents at the Skikda refinery during the period 2002–2013. The authors collected data on 44 accidents: fires (50%), explosions (20%), toxic product leaks (18%), electrical failures (4%), and others (8%). The years 2004 and 2005 were particularly marked by major incidents, and the frequency of accidents increased progressively from 2008 to 2013. These accidents were largely related to natural gas production (14%), crude oil (18%), heavy and light petroleum products (naphtha 11%, bitumen 7%, gas oil 11%, condensate 7%), natural gas liquefaction (3%), hydrogen (11%), hydrochloric acid (4%) and other prod-

[1]Laboratory of Chemical Processes and Environment, Uniiversity of Science and Technology of Oran Mohamed-Boudiaf USTOMB El Mnaouar, BP 1505, Bir El Djir 31000, Oran, Algeria.

[2]Laboratory of sciences and marine engineering, Uniiversity of Science and Technology of Oran Mohamed-Boudiaf USTOMB El Mnaouar, BP 1505, Bir El Djir 31000, Oran, Algeria.

*Corresponding author: K. Boumediene. E-mail Address: kadda.boumediene@univ-usto.dz.

ucts (7%).SM Tauseef et al. (2018) [2] investigated 28 major fire/explosion accidents at flammable liquid storage tank farms that occurred worldwide between 1995 and 2015.

The results showed that although industries often comply with tank-to-tank separation standards, many accidents rapidly spread to nearby tanks despite these "safe" distances. The causes included flammable vapour or liquid leaks (32%), lightning (21%), earthquakes (7%), explosions (14%), mechanical failures, human errors, and terrorist attacks (4%).The OISD-118, KLM, and HSG-176 standards applied in the study provided more realistic separation distances compared to those actually observed in accidents. The NFPA 30 Code (2024) [3] recommends safe separation distances between tanks to prevent fire or explosion risks. However, the actual separation distances during incidents were 2 to 4 times greater than the NFPA 30 recommendations in other words, the actual distances were only ½ to ¼ of those suggested by the code. This suggests that the NFPA 30 recommended distances might be insufficient to prevent certain accidents, since even larger distances did not prevent incidents. There may be a need to reassess or strengthen safety standards to better account for real-world scenarios or additional risk factors. Yasushi Oka et al. (2008) [4] explored the relationship between temperature rise and wind speed along the axis of an inclined fire plume. The study was conducted through experiments using a single fire source (a circular propane burner with a 0.2 m diameter) under crosswind conditions. Temperature and velocity were measured along the inclined fire plume axis and compared to calm conditions (no wind).

An empirical formula was developed to predict the speed of the inclined flame along the plume axis as a function of temperature rise and crosswind velocity. The results show good agreement between measured and calculated velocities, although some deviations occurred near the flame source. The formula is useful for estimating inclined flame plume velocity both with and without crosswinds.

S. Vasanth et al. (2014) [5] investigated Multiple Pool Fires (MPF), a phenomenon where two or more pool fires interact due to their proximity. Although common in chemical industries, MPFs have been underexplored.

Controlled experiments, mostly at small scale using CFD models, show that flames from nearby pool fires interact, resulting in increased flame height and enhanced thermal radiation compared to isolated fires. The burning rate increases due to thermal feedback between flames. When close enough, separate pool fires can merge into a single large flame.

Wang Wen-he et al. (2013) [6] conducted a numerical simulation of the thermal radiation field from a large-capacity crude oil storage tank fire. The aim is to analyse the characteristics of thermal radiation and assess fire and explosion risks for adjacent tanks. Using an empirical correlation, the flame height is calculated to be 75 m for an 80 m diameter tank. The simulation area had a radius of 300 m and a height of 171.8 m based on the safe distance needed to protect humans from a heat flux of 1255.2 W/m^2.

The study found that radiation intensity is highest near the flame and decreases with distance. Incident radiation intensity exceeded 200 kW/m^2 within 200 m of the flame center and dropped to 100 kW/m^2 at 250 m. Radiation is weaker at ground level than above the tank opening. In terms of risk, thermal radiation intensity ranged from 400 to 1000 kW/m^2 within a radius of 72 to 152 m, which could cause fires or explosions in nearby tanks if cooling measures are not promptly implemented.

S. Suard et al. (2013) [7] worked on predictive simulations of hydrocarbon fires in open and confined environments using the ISIS CFD Code. The main goal was to predict fuel mass flow rate under various configurations considering interactions between fuel and ambient gases.

The model is validated using heptane flames for three pool diameters (30, 60, and 100 cm) in open conditions. The study also show that reduced oxygen concentration significantly affects fuel mass flow. Results are compared with Peatross and Beyler's correlation, showing a nearly linear decrease in mass flow with oxygen reduction. Additional simulations of dodecane fires in mechanically ventilated compartments confirmed the model's ability to reproduce the fuel flow reduction when combustion products accumulate.

Sung-Kyu Lee and Jae-Yong Lim [8] study the impact of thermal radiation on weather patterns and the placement of flammable liquid storage tank. In reality, the regulation imposes separation lengths between tanks in order to prevent the cascading effect of fires. Although thermal radiation may be the cause of this effect, it must be carefully considered in the current Korean regulations. This study looks at three cases, two of which are based on weather conditions and one on a regulation. Risk analysis and assessment are calculated ALOHA program. Tank-farm configurations are resulting through the application of an optimization technique.

J. R. Welker et al. [9] investigated the effect of wind on the shape and tilt of diffusion flames particularly natural gas and liquid pool flames. The study proposed a correlation linking tilt angle (θ) to wind speed (u), flame diameter (D), and drag coefficient (Cf). It is based on experiments in a low-speed wind tunnel.

The correlation proved valid for natural gas flames, but challenges arose with liquid pool flames (e.g., hexane), due to their elliptical flame base and non-uniform tilt. While the correlation works well for natural gas, more complex modelling is needed for liquid flames due to their irregular geometry.

These findings are valuable for predicting fire hazards and designing safety measures especially in wind-affected environments.

The motivation for our study emerged from several major pool fire accidents that occurred at Sonatrach industrial facilities, particularly the Skikda industrial zone on 07/08/2013 (crude oil storage tank, RTO [10]).

Our approach involves a combination of statistical techniques, including descriptive analyses, correlation analyses, and predictive models such as multiple regression, Random Forest, and polynomial modelling to analyse and discuss potential correlations between meteorological conditions and thermal flux generated by a fire.

For this purpose, we exploited 17,000 data points collected over the past five years (note: 15,000 points are referenced in

the abstract, which refers to the filtered dataset after processing).

2. Description of the Facility and Immediate Environment.

The TNZ1 (Terminal Condensate Arzew), the subject of this study, covers a total area of 52 hectares. It is part of the RTO (Western Transport Region) located in Arzew, 35 km north-northeast of the city of Oran, and belongs to the TRC (Pipeline Transport) activity of the SONATRACH group.

This terminal includes seven floating roof tanks, whose characteristics are summarized in Table 1.

Table 1: Characteristics of the condensate storage tanks.

Tank	Diameter (m)	Height (m)	Bowl width(m)	Length width (m)	Tank Volume (m^3)	Bowl Volume (m^3)
R-851-852	57	15	112	153	38000	44125
R-853	57	15	108	153	38000	38000
R-854-855	67	17	160	220	60000	72265
R-856-859	67	17	109	241	60000	52538
R-860-861	67	17	100	215	60000	79550

Source: Authors.

Figure 1: Site layout of the NZ1 terminal platform.

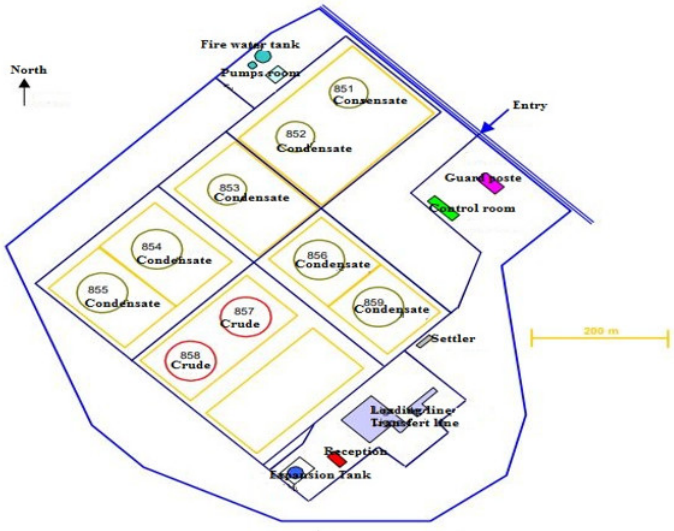

Source: Authors.

3. Methodology.

3.1. Collection and Exploration of Meteorological Data.

To carry out this study, we collected nearly 17,000 values (precisely 16,990) of meteorological data (temperature, wind speed, and air humidity) from the past six years (from January 1, 2019, to December 31, 2024) for the Arzew region, where the facility is located [11]. After checking for missing values, input errors, and unrecorded data from the National Meteorological Office (ONM), we retained 15,489 valid data points.

3.2. Calculation of Thermal Flux.

Microsoft Excel is the main tool used in this study to highlight correlations between different parameters and potential predictions.

The thermal flux associated with a tank fire, at thresholds of 3 and 5 kW/m^2, is calculated using the following relationship [12]:

$$\Phi = \Phi_0 \cdot F(r) \cdot \Gamma(r)$$

However, the parameters mentioned below are not directly part of the above equation:

- Φ_0 **(kW/m^2):** Emissive power
- **Γ(r):**Atmospheric transmissivity
- **Lf (m):**Flame length
- **Fr:** Froude number
- **Re:** Reynolds number
- **θ:** Inclination angle
- **Fv:** Vertical view factor
- **Fz:** Horizontal view factor
- **F:**View factor
- **Φ (kW/m^2):** Thermal flux

The emissive power Φ_0 is evaluated using the Mudan and Croce correlation [12]. This approach is based on data from tests conducted on fires ranging from 1 m to 80 m in diameter with various hydrocarbons (diesel, kerosene, and JP-5).
The emissive power of the flame is given by the following equation:

$$\Phi_0 = 20000 + 120000e^{-0.12\,Deq}$$

Where:

- **Deq:** The only variable in the formula, representing the equivalent diameter of the burning surface.

This correlation by Mudan and Croce is widely used in:

- TNO models,
- FRED software (Shell),
- UFIP, and
- PHAST (DNV).

The view factor F is determined based on:

- The dimensions and shape of the flame,
- The position and orientation of the target relative to the flame.

The cylindrical view factor derived from Mudan's work on flames modelled as an inclined cylinder (for wind speeds above 1 m/s) depends on:

- The equivalent diameter and flame length,
- The distance r between the flame and the target,
- As well as the inclination angle ξ of the flame.

$$F_m = \sqrt{F_h^2 + F_?^2}$$

With:

$$\begin{aligned}\pi F_v = {} & \frac{h\cos\xi}{S - h\sin\xi} \cdot \frac{h^2 + (S+1)^2 - 2S(1 + h\sin\xi)}{\sqrt{AB}} \\ & \cdot \tan^{-1}\left(\sqrt{\frac{A}{B}}\left(\frac{S-1}{S+1}\right)^{0.5}\right) \\ & + \frac{\cos\xi}{\sqrt{C}}\left[\tan^{-1}\left(\frac{hS - (S^2-1)\sin\xi}{(S^2-1)^{0.5}\sqrt{C}}\right) + \tan^{-1}\left(\frac{(S^2-1)\sin\xi}{(S^2-1)^{0.5}\sqrt{C}}\right)\right] \\ & - \frac{h\cos\xi}{S - h\sin\xi} \cdot \tan^{-1}\left(\left(\frac{S-1}{S+1}\right)^{0.5}\right)\end{aligned}$$

$$\begin{aligned}\pi F_H = {} & \tan^{-1}\left(\sqrt{\frac{S+1}{S-1}}\right) \\ & - \frac{h^2 + (S+1)^2 - 2(S + 1 + h\sin\xi)}{\sqrt{AB}} \tan^{-1}\left(\sqrt{\frac{A}{B}}\sqrt{\frac{S-1}{S+1}}\right) \\ & + \frac{\sin\xi}{\sqrt{C}}\left[\tan^{-1}\left(\frac{hS - (S^2-1)\sin\xi}{\sqrt{S^2-1}\sqrt{C}}\right) + \tan^{-1}\left(\frac{\sqrt{S^2-1}\sin\xi}{\sqrt{C}}\right)\right]\end{aligned}$$

With:

- h = L/R
- S = (r + R)/R
- R = Deq/2
- A = h^2 + (S+1)^2 – 2 h (S+1) sin ξ
- B = h^2 + (S-1)^2 – 2 h (S-1) sin ξ
- C = 1 + (S^2-1) $\cos^2\xi$

Deq: Equivalent diameter of the burning pool (circular fire).
Lf: Flame length or height (L)**ζ:** Flame tilt angle
The flame length Lis calculated under wind conditions > 1 m/s using Thomas' correlation.The tilt angle ζ is determined using the Welker and Sliepcevich correlation, with:
Fr: Froude number $F_r = \frac{u_w^2}{Deq.g}$
Re: Reynolds number $R_e = \frac{Deq.u_w.\,\rho_{air}}{\mu_{air}}$

- **ρ**$_{vap}$: Specific mass of the product in vapour phase at its boiling temperature (2.56 kg/m^3 for gasoline)
- **ρair**: Air density: 1.161 kg/m^3
- **μair**: Dynamic viscosity of ambient air (1.9×10^{-5} kg·m^{-1}·s^{-1})

Atmospheric transmissivity, which accounts for distance and humidity, is calculated using **Bagster's correlation [11]**:

$$\Gamma_r = 2.02 \cdot (HR \cdot T_{\mathrm{VAP}(H_2O)} \cdot r)^{-0.09}$$

3.3. Statistical Analysis and Modelling.

To visualize data distribution, descriptive statistical calculations (mean, median, standard deviation, variance, etc.) and representative graphs (histograms, scatter plots, etc.) were performed. The dispersion of the data is measured by variance and standard deviation. Correlation coefficients are calculated to assess the relationships between different variables.

Linear and non-linear correlation studies are performed using multiple regression analysis**,** which also serves as the basis for predictive modelling.

3.4. Validation.

Modelling results were validated using cross-validation methods. The performance of the model is assessed through analysis of Mean Squared Error (MSE)**.**

4. Results and Discussion.

4.1. Calculation of Central Tendency Measures.

Trends for the various meteorological parameters are summarized in Table 2.

Table 2: Measures of Central Tendency and Dispersion.

	Temperature (°C)	Wind Speed (m/s)	Humidity (%)	Emissive Power (kW/m²)	Atmospheric Transmissivity (ζ)	View Factor
Mean	20.06	15.84	75	20,13	0.159	2.35
Error	5.29	9,61	12.67	1,2577E-12	0.0044	0.59
Minimum	4.8	0.79	0. 5	20.13	0.155	0.49
Maximum	43.5	216	100	20.13	0.249	20.66

Source: Authors.

According to Table 2:

- **Temperature**: The recorded mean temperature is around 20.06°C. The standard deviation of 5.29 indicates moderate variability around the mean, reflecting seasonal or daily fluctuations. The minimum likely corresponds to cold conditions, while the maximum reflects extreme heat conditions.
- **Wind Speed**: The average wind speed is approximately 15.84 m/s (~57 km/h), indicating relatively strong winds. The standard deviation of 9.61 shows significant variability, with possible extremes ranging from calm to very violent winds. The maximum value of 216 m/s appears abnormally high and physically implausible (exceeding the most violent recorded tornadoes) suggesting a measurement or input error.
- **Humidity**: The recorded average humidity is 75%, a high value typical of coastal and humid climates where the air contains substantial water vapour. However, the standard deviation of 12.67 shows notable variability, alternating between dry and very humid conditions. The range spans from a minimum of 0.5% (exceptionally dry similar to desert or high-altitude air) to a maximum of 100% typical of saturated air during fog, rain, or condensation.

- **Emissive Power**: The average emissive power is 20.13 kW/m^2, an extremely high value with a near-zero standard deviation (1.2577 $\times 10^{-12}$ corresponding to a high-intensity heat source typical of a tank fire. The identical minimum and maximum values suggest a large fire surface area with a consistent radiative output.

- **Atmospheric Transmissivity**: The average transmissivity is 0.159 indicating a very opaque atmosphere. This low transmissivity can be attributed to persistent clouds, fog, or pollution, severely limiting thermal radiation transmission. The very low standard deviation (0.0044) suggests stable climatic conditions where atmospheric opacity is a consistent feature. The range between 0.155 and 0.249 supports the hypothesis of an environment saturated with aerosols, smoke or moisture obstructing radiative transfer.

- **View Factor**: The average view factor is 2.35, with a maximum of 20.66, highlighting the extreme radiative intensity of the thermal event. The standard deviation of 0.59 indicates high variability, influenced by:

  – The large surface area of the storage tank (expansive radiative source)

  – The tall, intense flames from condensate combustion

  – Thermal reflections from surrounding metallic structures

These factors amplify perceived radiation and underline the radiative hazard to personnel.

These measurements clearly reflect the exceptional intensity of a fire involving large-capacity hydrocarbon storage tanks. The analysis underscores the need to adapt classical theoretical models to extreme scenarios, encountered in major industrial accidents such as the case studied here.

4.2. Evaluation of Parameter Distributions.

Figure 2: Temperature distribution over the past six years.

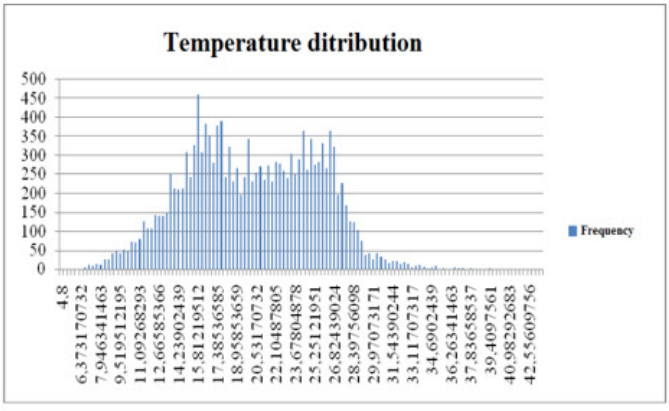

Source: Authors.

The results suggest high variability with an asymmetric distribution, indicated by a major peak around 15.81°C (with a very high frequency of 460) and several less pronounced peaks on the right. Peaks with frequencies above 30 are rare.

This indicates a positive skew, most data points are concentrated on the lower end (left side) with a few extreme high values on the right tail**.** Such a distribution does not follow a normal (Gaussian) law due to marked asymmetry.

Figure 3: Frequency distribution of humidity.

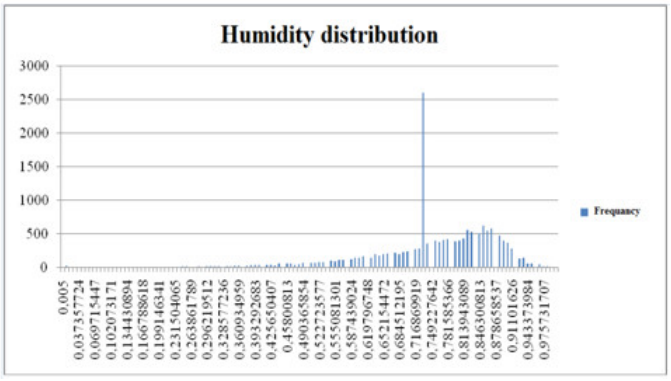

Source: Authors.

The distribution reveals prominent peaks and troughs, with several local maxima. The main value is observed between 0.733 and 0.741, totalling 2608 observations. Other noticeable peaks are spread across three intervals:

- From 0.44 to 0.47 (52–53 observations),
- From 0.55 to 0.63 (82–157 observations),
- From 0.82 to 0.83 (552–625 observations).

The observed asymmetry is complexed with a dominant extreme peak at 0.733, and data voids (zero frequencies) within intervals such as (0.021 to 0.037) and (0.498 to 0.507). This indicates a non-normal, multimodal distribution.

Figure 4: Distribution of wind speed, featuring a multimodal structure (multiple distinct peaks) and frequencies ranging from 0 to 2673 observations.

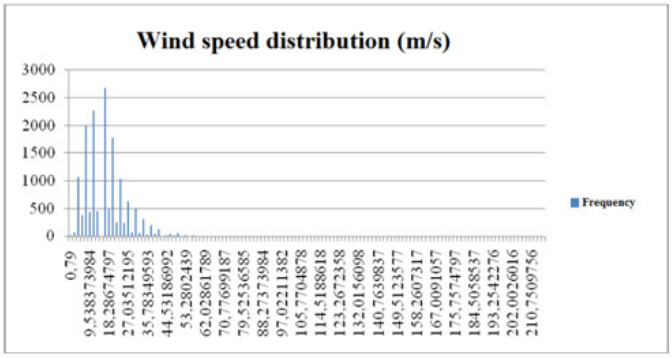

Source: Authors.

While the distribution extends up to 216 m/s, these extreme values are associated with very low frequencies and scattered intervals. In the 0–10 m/s range, two significant peaks occur at:

- 4.29 m/s (1065 observations)
- 7.79 m/s (1993 observations)

In the 10–20 m/s range, two other major peaks appear at:

- 11.29 m/s (2278 observations)
- 16.54 m/s (2673 observations)

Beyond 50 m/s, frequencies remain low and do not exceed 188. This reflects a complex, multimodal structure, with several sharp peaks, irregular decay toward higher values, and data voids suggesting threshold effects. Such a distribution requires advanced modelling adapted to multimodality.

Figure 5: Distribution of atmospheric transmissivity.

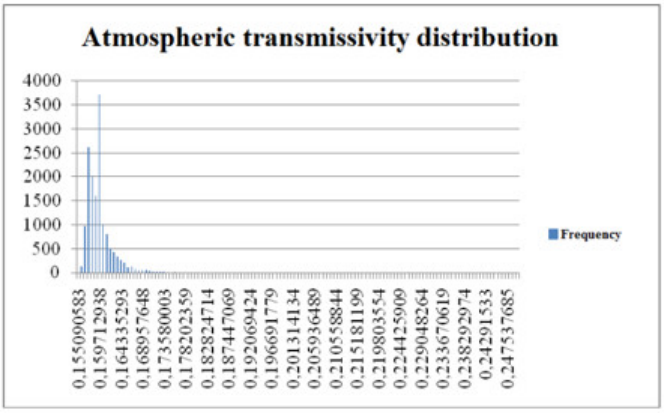

Source: Authors.

High frequencies are concentrated in the ranges:

- 2613 observations between 0.1574 and 0.1589
- 3729 observations between 0.1597 and 0.1605

The concentration of data in specific intervals suggests an asymmetric and multimodal distribution.

Figure 6: Distribution of the view factor.

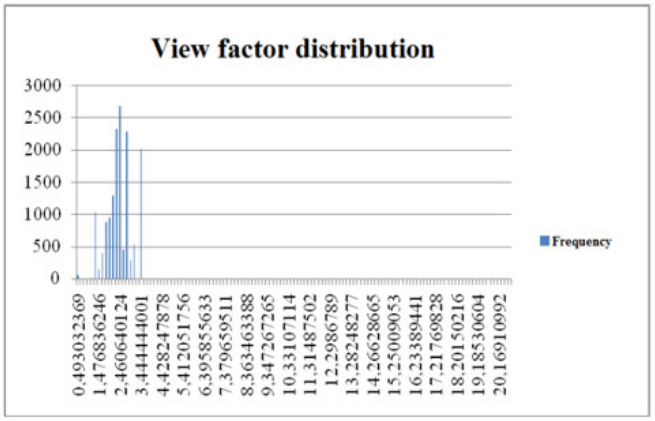

Source: Authors.

Most of the domain corresponds to zero frequencies, except for a few significant peaks, notably:

- 2675 observations (2.460 to 2.624)
- 2322 observations (2.296 to 2.460)
- 2004 observations (3.444 to 3.608)
- 2278 observations (2.788 to 2.952)

These results describe an asymmetric and plurimodal distribution, requiring an appropriate modelling approach.

Figure 7: Distribution of heat flux, exhibiting multiple distinct peaks separated by null-frequency zones, clearly indicating a multimodal phenomenon.

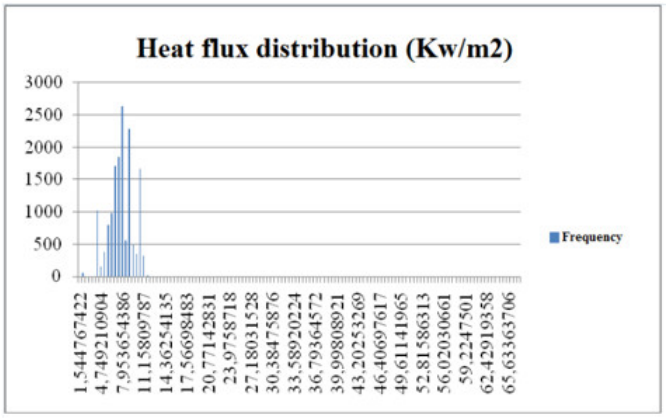

Source: Authors.

The highest frequencies include:

- 1024 observations (4.215 to 4.749)
- 2641 observations (6.885 to 7.953)
- 2285 observations (9.021 to 9.555)
- 1675 observations (14.362 to 14.896)

4.3. Correlation Analysis.

Table 3 presents the **correlation matrix** between various variables, including:

- Temperature (°C)
- Wind speed (m/s)
- Emissive power (kW/m^2)
- Atmospheric transmissivity (ζ)
- Flame length (m)
- Tilt angle
- View factor
- Heat flux

Table 3: Correlation matrix.

	T (°C)	Hum (%)	v vent (m/s)	ϕ0 (kW/m²)	ζ	L_f (m)	Tilt Angle	F	ϕ
Temperature (°C)	1	-0,139	0,089	1,77E-14	0,113	-0,151	0,109	-0,0065	0,00548
Humidity (%)	-0,139	1	-0,124	-3,23E-13	-0,796	0,1068	-0,0395	0,0479	-0,0317
Wind Speed (m/s)	0,089	-0,124	1	3,40E-14	0,132	-0,835	0,267	-0,381	-0,371
Emissive Power ϕ_0 (kW/m²)	1,77E-14	-3,23E-13	3,40E-14	1	-5,08E-13	-7,41E-13	-4,00E-12	1,38E-13	-8,36E-16
Transmissivity Atmospheric ζ	0,113	-0,796	0,132	-5,08E-13	1	-0,0939	0,0132	-0,0682	0,0186
Flame Length L_f (m)	-0,151	0,1068	-0,835	-7,41E-13	-0,0939	1	-0,593	0,183	0,175
Tilt angle (θ)	0,109	-0,0395	0,267	-4,00E-12	0,0132	-0,593	1	0,624	0,625
View factor F	-0,0065	0,0479	-0,381	1,38E-13	-0,0682	0,183	0,624	1	0,995
Heat Flux ϕ (kW/m²)	0,00548	-0,0317	-0,371	-8,36E-16	0,0186	0,175	0,625	0,995	1

Source: Authors.

This, a weak negative correlation is observed between temperature and humidity (-0.139), as well as between temperature and flame length (-0.151). A slight increase in temperature tends to reduce both of these parameters. Practically, there is no significant relationship between temperature and emissive power (1.77×10^{-14}), view factor (-0.0065), or heat flux (0.00548). However, a slightly positive relationship is noted with wind speed (0.089), atmospheric transmissivity (0.113), and inclination angle (0.109). A marginal increase in temperature could be accompanied by a slight rise in these three parameters.

It is important to note that the near-zero correlation between temperature and heat flux reflects the marginal effect of ambient temperature on heat flux. A tank fire is primarily driven by the combustion of condensates (hydrocarbons). The intensity of which does not significantly depend on moderate variations in ambient temperature.

Humidity shows weak negative correlations with wind speed (-0.124), inclination angle (-0.0395), and heat flux (-0.0317). No significant relationship is observed with emissive power (-3.23×10^{-13}) or with the view factor (0.0479). The correlation with flame length is weakly positive (0.1068). On the other hand, a strong negative correlation is recorded between humidity and atmospheric transmissivity (-0.796) indicating an increase in humidity leads to a significant decrease in transmissivity.

The very weak negative correlation between humidity and heat flux suggests that higher humidity may slightly reduce heat flux as humid air absorbs part of the thermal radiation, thereby attenuating the emitted flux. It may also alter the combustion kinetics by slowing it down through oxygen dilution.

$$\begin{aligned}\Phi = & -3.8853 + 3\cdot10^{-4}T - 0.4422H - 7\cdot10^{-4}V \\ & - 9\cdot10^{-15}\Phi_0 + 27.1059\xi - 9\cdot10^{-4}L_F \\ & - 8.8\cdot10^{-3}\theta + 3.2064F\end{aligned}$$

Wind speed presents a moderately negative correlation with the view factor (-0.381) and heat flux (-0.371), and a strong negative correlation with flame length. It shows no correlation with emissive power (3.40×10^{-14}) and weakly positive correlations with inclination angle (0.267) and atmospheric transmissivity (0.132).

The correlation between wind speed and heat flux indicates that higher wind speeds reduce heat flux through forced convection, which dissipates heat and cools the surface of the tank. Strong winds can also disperse flammable vapours, limit fire intensity and alter flame geometry, thereby reducing the density of radiative energy perceived. The strong relationship between wind speed and flame length is explained by flame dissipation due to blowing, which also, contracts the flame length and thus reduces the surface exposed to fire.

Therefore, wind is considered the dominant meteorological factor in modulating the fire's heat flux while humidity plays an indirect role through atmospheric transmissivity (ζ) which is strongly linked to combustion.

4.4. Model reliability study.

To determine the credibility of the established model, a calculation of regression and variance statistical parameters is necessary.

Table 4: Gathers the different statistical parameters of the regression.

Statistic	Value
Multiple R	0.9998
R Square (R2)	0.9996
Adjusted R Square	0.9995
Standard Error	0.03759
Observations (n)	15,316

Source: Authors.

The multiple determination coefficient (R) measures the correlation between actual and predicted values. The value of 0.9998, which is very close to 1, indicates a very strong correlation between the explanatory variables and the dependent variable. R^2 measures the proportion of variance in the dependent variable explained by the explanatory variables. The value of 0.9996 means that the model explains 99.96% of the variance. This indicates an almost perfect fit of the model to the data.

The adjusted R^2 takes into account the number of explanatory variables in the model. It is slightly lower than the standard R^2 because it penalizes the addition of non-significant variables. A value of 0.9995 confirms that the model is highly efficient even after adjustment.

The standard error measures the accuracy of the model's predictions. A low value of 0.0375, which is close to 0 indicates that the predictions are very close to the observed values, confirming the high precision of the model. The model is trained on 15,319 observations that is a very large sample. This strengthens the reliability of the results.

The value of variance parameters are presented in table 5.

Table 5: Variance parameters.

	Degree of Freedom	Sum of squares	Mean of squares	F	p-value
Regression	8	55867,48022	6983,435027	5646171,79	0
Residuals	15308	21,63841321	0,001413536		
Total	15316	55889,11863			

Source: Authors.

1. **Regression (Model)**
   The degree of freedom, determined, indicates that the model uses eight explanatory variables (temperature, humidity, wind speed, emissive power, atmospheric transmissivity ζ, view factor, flame length Lf, and inclination angle θ).
   The sum of squares**,** equal to 55,867.48**,** is very high, which suggests that the included variables capture a large part of the variation in the dependent values.The value of the mean squares**,** 6,983.44, is adequate with the degree of freedom.Regarding the F-statistic and the p-value, their respective values 5,646,171.79 and 0 indicate that the model is extremely significant**.**
2. **Residuals (Errors)**
   The degree of freedom**,** 15,308**,** means that the number of actual observations is slightly lower than the number of estimated parameters.
   The residual sum of squares, 21.64, is extremely low compared to the regression sum of squares, indicating an almost perfect fit.
   The low residual mean square**,** 0.00141**,** suggests that the predicted model is virtually error-free.

4.5. Study of multi collinearity in the matrix.

According to the correlation analysis (Table 2), we observed that there is a relatively high correlation (0.624) between the inclination angle and the view factor (F). This could indicate a certain form of multi collinearity between these two variables.

Moreover, moderate correlations are observed between wind speed (-0.835) and flame length, as well as with the inclination angle (0.267). These are not strong enough to cause serious multi collinearity issues.

The other correlations are weak. For example, temperature and humidity show a correlation of -0.139, indicating an absence of collinearity between these variables.Based on the correlation matrix, there is no significant multi-collinearity in the overall data but there are signs of moderate redundancy between certain variables, as is the case between inclination angle, view factor, and heat flux.

We can therefore conclude that there is no significant multi collinearity that could lead to problematic situations in our model.

4.6. Prediction study.

The prediction study is based on the comparison between the actual values and those predicted by the model.

A good prediction means that the points representing the actual values must be close to those representing the predicted values.

Figure 8: Presents a comparison graph between these values using the multiple regression models.

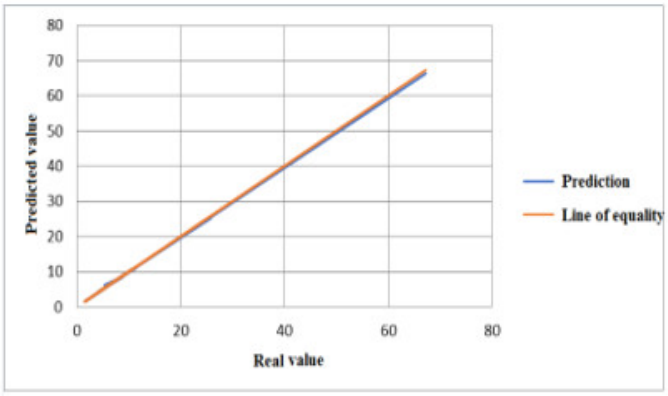

Source: Authors.

Practically, the two curves are identical (superimposed) and reflect the perfect accuracy of our model. Thus, the predicted values exactly match the actual values.

The horizontal line (blue) represents the ideal case where the errors are zero and the predictions are perfect. When the points are close to this line, it means that the predicted model is adequate**.**

Figure 9: Displays the residual dispersion, i.e., the difference between actual values and those predicted by the model.

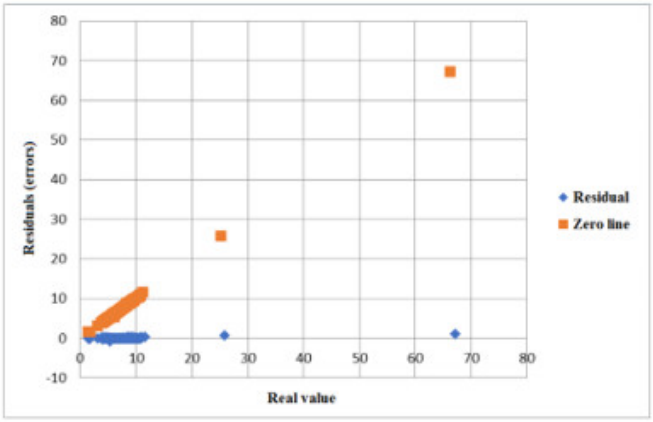

Source: Authors.

Moreover, a homogeneous dispersion around zero indicates that the model gives errors in a balanced manner.

If the errors increase according to the actual value (fan effect), this may indicate that the model works better for some value ranges than for others.

A numerical analysis of the errors yields the following findings:

- Mean ≈ 0.0003 → the errors are balanced around zero,

which means that the model neither systematically underestimates nor overestimates.

- Standard deviation ≈ 0.0407 → the errors are on average low, which indicates good model accuracy.
- Min: -0.7025 / Max: 0.9937 → the largest negative and positive errors indicate that in some cases, the model is wrong by up to ±0.7 relative to the unit.

Thus, we can conclude that:

- The model is well calibrated, as the mean of errors is close to zero.
- There is no systematic bias (no clear trend in the errors).
- Some significant errors exist, but they are rare and do not question the overall quality of the model.

4.7. Study of variable importance.

Table 6: Importance calculation of variables related to the Random Forest model.

Variable	Importance
View Factor	0,94973502
Wind Speed (m/s)	0,01877864
Inclination Angle	0,01339145
Flame Length (m)	0,00943672
Atmospheric Transmissivity (ζ)	0,00563769
Humidity (%)	0,00300812
Temperature (°C)	1,2359E-05
Emissive Power ϕ_0 (kW_m^2)	0

Source: Authors.

The most important variable is the view factor F. This variable has an importance of 0.9497, which means it has the greatest influence on the heat flux.

A variation of F causes a significant change in Φ. As a result, it is essential in the model and must be retained.

Other variables have notable but lesser influence than F.

We can mention wind, inclination angle, and flame length, which have respective importance of 0.0188, 0.0134, and 0.0094.

These parameters contribute to the prediction of Φ, but their influence is less dominant.Their removal could slightly affect the accuracy of the model.

However, temperature is the variable that has almost no impact on Φ and can be removed without affecting the model's accuracy.

Its importance is very low and close to zero.

Conclusions.

This study is based on a large dataset covering several years of operation from one of the most active complexes in the industrial zone of Arzew. Several parameters were studied with the aim of understanding the effect of meteorological factors on the heat flux from a storage tank fire (tank fire).

It was demonstrated that the view factor (F) is the most important parameter in predicting the heat flux (impact distance), while highlighting that the current practices used in the study area (RTO) are completely inadequate, since the impact distance adopted in the area is considered fixed throughout the year and in all scenarios.

References.

[1] Samia Chettouh, Rachida Hamzi, Khemissi Benaroua, *Examination of fire and related accidents in Skikda Oil Refinery for the period 2002–2013*, *Journal of Loss Prevention in the Process Industries*, 2014.

[2] S.M. Tauseef, Tasneem Abbasi, V. Pompapathi, S.A. Abbasi, *Case studies of 28 major accidents of fires/explosions in storage tank farms in the backdrop of available codes / standards / models for safely configuring such tank farms*, *Process Safety and Environmental Protection*, 2018.

[3] NFPA 30, Flammable and Combustible Liquids Code, 2024 Edition Paperback.

[4] Yasushi Oka, Osami Sugawa, Tomohiko Imamura, *Correlation of temperature rise and velocity along an inclined fire plume axis in crosswinds*, *Fire Safety Journal*, Vol. 43 (2008), pp. 391–400.

[5] S. Vasanth, S.M. Tauseef, Tasneem Abbasi, S.A. Abbasi, *Multiple pool fires: Occurrence, simulation, modeling and management*, *Journal of Loss Prevention in the Process Industries*, Center for Pollution Control and Environmental Engineering, 2014.

[6] WANG Wen-he, XU Zhi-sheng, SUN Bao-jiang, *Numerical Simulation of Fire Thermal Radiation Field for Large Crude Oil Tank Exposed to Pool Fire*, *Procedia Engineering*, Vol. 52 (2013), pp. 395–400.

[7] Sylvain Suard, Ahmed Kacem, Hélène Martin, Bernard Porterie, *Predictive simulations of a hydrocarbon fire in open and confined environments*, *21st French Congress of Mechanics (CFM 2013)*, Aug 2013, Bordeaux, France. Hal-03441401.

[8] Sung-Kyu Lee and Jae-Yong Lim, Important safety considerations for arrangement of flammable storage tanks: Thermal radiation effects with meteorological conditions. Process Safety Progress Volume 42, Issue 4 December 2023 Pages 752-762.

[9] R. Welker, O.A. Pipkin, C.M. Sliepcevich, *The Effect of Wind on Flames*, University of Oklahoma at Norman, [year not specified].

[10] *RTO Hazard Study* (Étude de danger RTO), [internal document].

[11] *National Office of Meteorology* (Office National de la Météorologie), Algeria.

[12] *Knowledge and Tool Formalization in the Field of Major Industrial Risks (DRA-76)/Ω-2: Industrial Fire Modeling*, DRA-14-141478-03176A, 2014.